Contents list available at CBIORE journal website

International Journal of Renewable Energy Development

Journal homepage: https://ijred.cbiore.id

Research Article

Assessing the potential tsunami source of the Manila trench at the Bengkayang nuclear power plant site in Kalimantan using topographical details

Sugeng Pribadi[a], Widjo Kongko[b], Nurkhalis Rahili[b]*, F. Fauzi[a], Hadi Suntoko[c], Sapto Nugroho[b], S. Sunarko[d], Telly Kurniawan[a], Euis Etty Alhakim[c]

[a]*Meteorological, Climatological, and Geophysical Agency, Indonesia*

[b]*Research Center for Hydrodynamic Technology, National Research and Innovation Agency, Indonesia*

[c]*Research Center for Nuclear Reactor Technology, National Research and Innovation Agency, Indonesia*

[d]*Indonesian Nuclear Technology Polytechnic, National Research and Innovation Agency, Indonesia*

Abstract. Tsunamis pose a significant threat to the construction of Nuclear Power Plants. Therefore, it is necessary to carry out a comprehensive study regarding the potential threat of tsunamis and mitigation measures using detailed data at prospective locations. This assessment is a prerequisite for effective environmental impact planning and analysis. To determine the suitability of a prospective location, careful consideration of natural factors, including earthquakes as triggers for tsunamis, is essential. The main objective of this tsunami research is to assess the level of safety of potential locations against tsunami hazards and develop appropriate mitigation strategies. This research uses the Cornell Multigrid Coupled Tsunami (COMCOT) tsunami modeling technique. This modeling approach utilizes topographic and bathymetric data obtained through extensive field surveys. In addition, this research aims to determine the maximum tsunami height in the inundation area and identify potential tsunami hazards arising from various scenarios related to the active tectonic potential of the Philippine Manila Trench. The Bengkayang Gosong Beach area and West Kalimantan are among the candidate locations that may be affected with the estimated tsunami height being between 0.48 meters and 0.62 meters. The tsunami arrival time was between 9 hours 10 minutes to 9 hours 24 minutes. These findings play an important role in conducting comprehensive risk assessments for nuclear power plant development, ensuring that necessary steps are taken to reduce potential hazards associated with tsunamis.

Keywords: nuclear power plants, tsunami, modeling, COMCOT, Manila Trench

Received: 10th Sept 2023; Revised: 8th Nov 2023; Accepted: 6th Dec 2023; Available online: 29th Dec 2023

1. Introduction

Tsunamis are marine disasters that threaten coastal areas, including nearshore nuclear reactors. Tsunamis are large waves that occur when parts of the ocean floor change their geometry due to plate movement, volcanic eruptions, or underwater landslides (Diposaptono and Budiman, 2006). The main focus for many industrial facilities near the coast is the threat of tsunamis. Industries like Nuclear Power Plants (NPP) prioritize safety, so when determining the feasibility of a site, it is crucial to consider natural factors, including the earthquake source that can trigger a tsunami. In 2019, the West Kalimantan provincial government proposed the Gosong Beach area in the Sungai Raya District, Bengkayang, West Kalimantan (Fig. 1), as a candidate site for a NPP. Given the high-risk nature of nuclear facilities, constructing a NPP must prioritize a high safety factor. One crucial aspect of site safety is assessing the potential geological threats and the risk of coastal flooding caused by tsunamis, which can disrupt the installation and operation of the reactor (BAPETEN, 2018). In line with Law No. 24 of 2007 concerning Disaster Management (UU, 2007) enacted by the President of the Republic of Indonesia, it is necessary for this infrastructure development study to incorporate preventive and countermeasures for managing earthquake and tsunami disasters. These measures should be implemented before and after a disaster to reduce the associated risks effectively.

Active faults and undersea volcanoes can serve as sources of earthquakes that generate tsunamis. The West Kalimantan region, particularly at Gosong Beach in Bengkayang Regency, West Kalimantan, has a minimal earthquake record due to its distance from active faults and tectonic activities. Nevertheless, according to Regulation No. 6/2014 (BAPETEN, 2014). It is necessary to assess the potential tsunami hazards originating from earthquake sources in the identified potential NPP site. Additionally, Presidential Regulation No. 79 of 2014, which pertains to the National Energy Policy (KEN), emphasizes including nuclear energy within the national energy system and underscores the importance of site preparation by applicable safety regulations (PP, 2014).

* Corresponding author
Email: nurkhalis.rahili@gmail.com (N. Rahili)

https://doi.org/10.14710/ijred.2024.57967
ISSN: 2252-4940/© 2024.The Author(s). Published by CBIORE

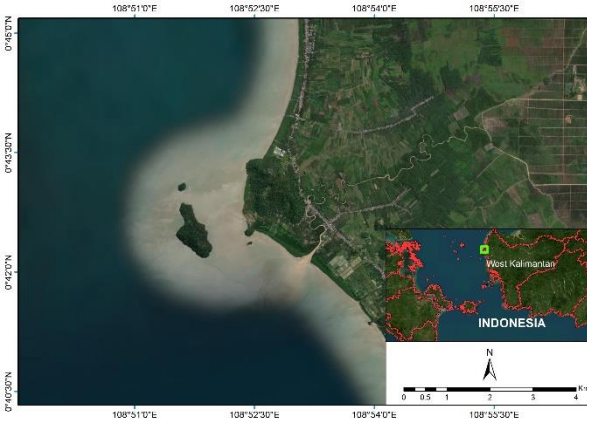

Fig. 1 Map of the candidate site for a Nuclear Power Plant.

In light of the Tohoku Earthquake that occurred in Japan on March 11, 2011, with a magnitude Mw of 9.1, causing a devastating tsunami reaching a height of 14 meters, which breached the sea wall and inundated the reactor building of the Da-ichi Fukushima nuclear power station located 72 kilometers from the tsunami source in the Pacific Ocean (Lipscy *et al*., 2013), it is imperative to conduct research activities to prepare the NPP at Gosong Beach against the threat of a tsunami hazard.

Based on population data for 2018, the total population around the prospective NPP Pantai Gosong site at a radius of 5 km is 5,199 people, with the largest population in the River Desa Raya, which has a population of 3,473 and the least is Karimunting Village with a total of 769 inhabitants. The density of the population is 177 people/km^2 (Alimah *et al,* 2021). The demographic condition of the residents of Gosong Beach is quite vulnerable if a disaster occurs to the NPP when it is operating so it requires adequate mitigation planning.

This research aims to assess the safety level of the NPP site in terms of potential tsunami hazards and develop appropriate mitigation measures. Additionally, this research aims to determine the height of tsunamis taking into account the effect of inundation areas and identify potential tsunami hazards associated with existing earthquake sources. Furthermore, areas prone to tsunami disasters must implement preventive and mitigation measures to address earthquake-related hazards before and after such events occur. These measures are essential for minimizing the risks associated with these disasters. When selecting a suitable site for a nuclear power plant, it is advisable to choose an area that has not experienced coastal flooding caused by tides or tsunamis in the past. This criterion improves the site's suitability and reduces the potential impact of coastal hazards on the facility.

2. Methods

2.1. Tsunami

In order to conduct tsunami modeling, numerical modeling techniques can be employed. The study of seawater's motion properties requires marine hydrodynamic models. Hydrodynamics involves the exploration of governing equations and numerical methods for tsunami modeling.

The linear and nonlinear shallow water equations can be described in both Cartesian and Spherical coordinates. The nonlinear shallow water equation affected by bottom friction effects is sufficient to describe flow motion in the coastal zone (Kajiura and Shuto, 1990; Liu *et al*., 1994). The Cartesian coordinate system has three axes: x, y, and z, resulting in the formation of Cartesian spaces such as x-y, x-z, and y-z as well as the eight octants. Conversely, the typical spherical coordinate system utilizes three parameters: the radial distance R, the polar angle ψ, and the azimuth angle φ (Wang and Power, 2009). The equations for spherical and Cartesian coordinates can be formulated as follows:

$$\frac{\partial \eta}{\partial t} + \frac{1}{Rcos\varphi}\left\{\frac{\partial P}{\partial \psi} + \frac{\partial}{\partial \varphi}(cos\, cos\, \varphi Q)\right\} = -\frac{\partial h}{\partial t} \quad (1)$$

$$\frac{\partial P}{\partial t} + \frac{gh}{Rcos\varphi}\frac{\partial \eta}{\partial \psi} - fQ = 0 \quad (2)$$

$$\frac{\partial Q}{\partial t} + \frac{gh}{R}\frac{\partial \eta}{\partial \varphi} - fP = 0 \quad (3)$$

where variable η represents the elevation of the water surface, the volume flux of the fluid material in the West-East (X) and South-North (Y) directions is denoted by (P, Q) respectively, meanwhile parameters (φ, ψ) correspond to Earth's latitude and longitude, R represents the radius of the Earth, and the acceleration due to gravity is denoted by g, h represents the water depth, additionally, a term accounting for transient seafloor movement can be incorporated to simulate tsunamis triggered by landslides.

The f value represents the coefficient of the Coriolis force due to the Earth's rotation and can be calculated using the following equation:

$$f = 2\Omega \sin\varphi \quad (4)$$

where Ω represents the rotation of the Earth, and φ is the latitude. When conducting tsunami modeling in shallow water, the influence of Earth's rotation is relatively small within the narrow region of interest. Therefore, the shallow water equations in Cartesian coordinates can serve as a suitable reference for modeling, and they can be expressed as follows:

$$\frac{\partial \eta}{\partial t} + \left\{\frac{\partial P}{\partial x} + \frac{\partial Q}{\partial y}\right\} = -\frac{\partial h}{\partial t} \quad (5)$$

$$\frac{\partial P}{\partial t} + gh\frac{\partial \eta}{\partial x} - fQ = 0 \quad (6)$$

$$\frac{\partial Q}{\partial t} + gh\frac{\partial \eta}{\partial y} + fP = 0 \quad (7)$$

2.2. COMCOT Modelling

Tsunami numerical modeling using the Cornell Multi-grid Coupled Tsunami (COMCOT) model is based on the Shallow Water Equations (SWE). Numerical models based on SWE offer superior performance as they fulfil technical requirements such as hydrodynamics, alignment with real-world scenarios, operational conditions, and scientific evaluation (Dao and Tkalich, 2007). COMCOT shares similarities with TUNAMI-N2, including the model structure, numerical scheme, programming language, and the use of Manning roughness. The latest version of COMCOT, V1.7, has been enhanced with a multi-grid system to improve accuracy and efficiency, and its documentation is publicly available (Wang and Power, 2009).

Tsunami sources in this study utilized a fault model that integrates empirical scale laws and inversion models of tsunami waveforms, as established by Mansinha and Smylie (1971). The

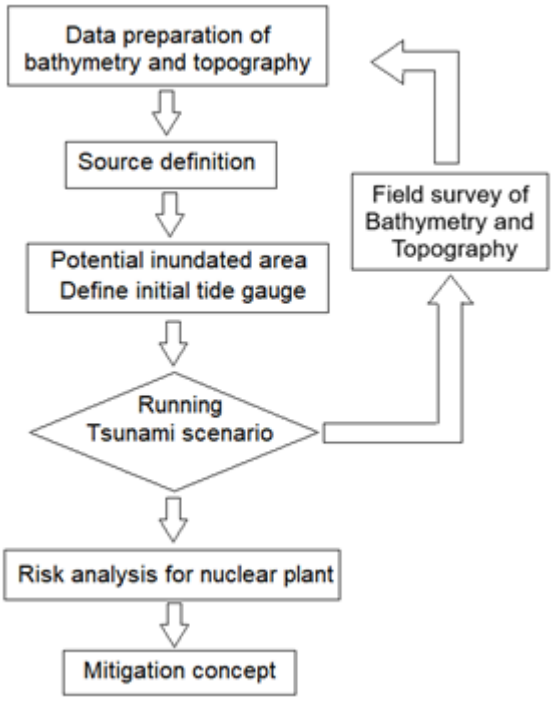

Fig. 2 Diagram for tsunami modeling work chart.

earthquake potential was systematically divided into 33 fault segments, following the methodology outlined by Blaser *et al*. (2010). This approach incorporates precise calculations derived from diverse regression methods based on extensive global data, providing a comprehensive scaling relationship for determining the length, width, and moment magnitude of thrust, normal, and strike-slip faults in both oceanic and continental regions. The tsunami source scenarios in this research follow a deterministic approach, where earthquake and tsunami experts have predefined the tsunami source model (PUSGEN, 2018). Our tsunami modeling employs detailed data with a resolution as fine as 1 m to attain optimal results. Additionally, beyond the utilization of geometrical features derived from detailed bathymetric and topographic data at the study location, we conduct a thorough analysis of other parameters, such as tsunami wave velocity. This approach enables a more detailed examination of the threat aspect in the water-cooling system area and its associated infrastructures. In contrast to previous studies that modeled tsunamis from their sources, propagation, and estimated arrival to sea surface height within the numerical domain, our study goes further by focusing on the Nuclear Power Plant candidate. However, it should be noted that the previous study did not delve into a more detailed evaluation of this specific focal point. The stages of modeling work are described in the diagram in Fig. 2.

2.3. Initial Tide Gauge

In order to obtain the height and arrival time of the tsunami in the vicinity of Gosong Beach, an initial tidal point was established, starting from the farthest location and progressing towards the nearest location. These tidal points' positioning varied to assess the response of the tsunami waves in different areas, including the open sea, areas near small islands, and the vicinity of Gosong Beach Bay. Placing tidal points on the mainland would result in overlapping signals on the tide gauge, rendering the modeling process unsuccessful. Therefore, artificial stations were strategically positioned on the high seas. These stations measure the height and arrival time of the tsunami at those specific locations, providing valuable data before its landfall (Pribadi *et al.,* 2021).

2.4. Data Acquisition and Assimilation

As a basis for making tsunami modeling, sea and land data are needed. The availability of detailed data is absolutely necessary to produce a quality tsunami hazard map (Latief, 2013). Bathymetry and topographic maps. A bathymetry map is a map that describes the waters and their depth. A topographic map is a type of map characterized by its large scale and detail, usually using contour lines in modern mapping. Topographic maps are detailed and accurate graphical representations of the state of the world on a landmass.

For tsunami modeling, the first, second and third simulation starts from the initial domain, namely the wide-scale sea surface of the General Bathymetric Chart of the Oceans (GEBCO) with a resolution of 480 meters. GEBCO provides the most authoritative and publicly available bathymetric data set for the deep world's oceans. The fourth and fifth domains were taken from the National Bathymetry Geospatial Information Agency (BIG) and the National Waters Bathymetry (BATNAS) with a resolution of 180 meters. The source of BATNAS data acquisition is based on BIG, NODC, BODC, LIPI, BPPT, P3GL and global data. Horizontal and vertical references are WGS84 and MSL.

The sixth domain is the combination of BATNAS and Digital Elevation Model (DEMNAS) topographic map with a resolution of 8 meters. DEMNAS data sources were obtained from IFSAR, TerraSAR-X, and ALOS PALSAR. DEMNAS references for horizontal and vertical are WGS84 and EGM2008. The last domain is a combination between the sixth domain and field survey observation data. The stages of setting the resolution of each modeling domain are described in Table 1.

2.5. Topography and Bathymetry field survey

Research on determining the location of potential NPP sites in Bengkayang has carried out topographic and bathymetric field surveys around Gosong beach in 2021 to 2023. Based on geological observations, Gosong has a fairly shallow depth evidenced by the turbidity of light brown sea water. The dominant process is deposition due to coastal erosion which has sedimentary rock units in the form of sandstone and alluvial. The slope of the beach slope is in the range 3° – 15°. Intensive erosion processes occur in coastal areas between Singkawang City and the coast of Gosong, and are characterized by the formation of an erosion escarpment as high as ± 1.5 m (Suntoko *et al,* 2021). This condition requires verification by a field survey with topographical and bathymetric measuring equipment.

Topographic surveying is the process of measuring and mapping the shape of the earth's surface, including contours, elevations and other features such as hills, valleys and rivers.

Table 1
Resolution of grid size domain.

Domain	Data ref.	Res (degree)	Res (m)
1, 2, 3	GEBCO/G	0.00416667	463
4, 5	BATNAS/B	0.00166667	180
6	B, DEMNAS/D	0.00006312	8
7	B, D, Field Survey	0.00000898	1

Fig. 3 Topography and Bathymetry field survey

Topographic maps are useful in identifying the physical characteristics of an area quantitatively such as geographic coordinates and surface elevation. The Global Navigation Satellite System (GNSS) is a fast method that uses satellite signals to quickly determine the coordinates of many measurement points with high accuracy (Schloderer et al, 2010). Topographic measurements in this study also add UAV drone or Unmanned Aerial Vehicle equipment, namely unmanned aircraft to measure coordinates and altitude so that work can take place faster and have a wider coverage area.

Retrieval of ocean shallow depth measurement data can be done using an echo sounder. To measure coastal bathymetry, in this study using the Multibeam Echo Sounding (MBES) and Light Detection and Ranging (LIDAR) method. MBES uses an array of beams from sonar sensors that generate sound pulses to the ocean floor. Echoes reflected back from the ocean floor are then recorded to measure depth. This method provides high-resolution bathymetry data and enables accurate mapping. LIDAR uses laser pulses but is emitted from aircraft or ships to the surface of the sea. The reflected laser pulse is then recorded to measure the shallow depth (Webb, 2017). The detailed topography in this study is the result of integrating data from BATNAS, DEMNAS, UAV, and field surveys to produce high-resolution maps. To obtain a high-resolution map, the data has been processed by smoothing and filtering satellite data from SRTM. Subsequently, it was combined with DEM data for the Gosong beach area. The resulting map product is a grid with uniform spacing of a 3 x 3 m raster. High resolution maps are capable of providing accurate and important results of modeling tsunami inundation and run-up. Meanwhile, previously recognized data has a rough resolution (Schlurmann *et al*, 2011).

Tsunami inundation model is very sensitive to height data and depends on detailed topography and bathymetry data. High resolution bathymetry data can be obtained by combining the global GEBCO dataset used in deep water (90 m resolution) with additional higher resolution naval chart data (DISHIDROS) in shallow water areas. Meanwhile, topographic data uses digital IFSAR data in the air (owned by BIG) with a horizontal distance of 5 m resolution and a vertical accuracy of 3 m (Griffin *et al*, 2016). Topographical and bathymetric field survey work can be seen in Fig. 3.

2.6. Earthquake Source

Indonesia sits at the convergence of multiple tectonic plates, including the Indian Ocean Plate and the Eurasian Plate. This intersection occurs along the west coast of Sumatra, the south coast of Java, Bali, and Nusa Tenggara, making these regions prone to earthquakes and highly vulnerable to the threat of tsunamis (Bock *et al,* 2003; Pribadi, *et al*., 2013). The collision between the northward-moving Indo-Australian Plate and the south-eastward-moving Eurasian Plate, at respective speeds of approximately 7 centimetre/year and 0.4 centimetre/year, contributes to these seismic activities. While Kalimantan Island is situated far from the collision zone, it still experiences tectonic processes that have given rise to geological structures like folds and faults. Some of these faults are active and can be observed through seismic events (Supartoyo, 2017).

The Bengkayang area and its surroundings are located within the tectonic framework of the Sunda Shelf. This region is crossed by various geological structures, resulting in the exposure of Mesozoic-aged rocks at the surface. The measurement data collected in the study area indicates fluctuating changes in sediment supply, ranging from transitional environments to the sea (Hakim and Setijadi, 2021).

Based on data from the Global Historical Tsunami Database, accessible through the National Oceanic and Atmospheric Administration (NOAA) (http://ngdc.noaa.gov), a total amount of 119 earthquakes around Kalimantan and Philippine with tsunami potential were recorded from 1605 to 2023 in the region between 5° South and 20° North, and 108° East to 129° East, shown in Fig. 4. However, in Kalimantan, there are no significant earthquakes that have caused tsunamis. The tectonic activity in the western region of Kalimantan Island is relatively low. The

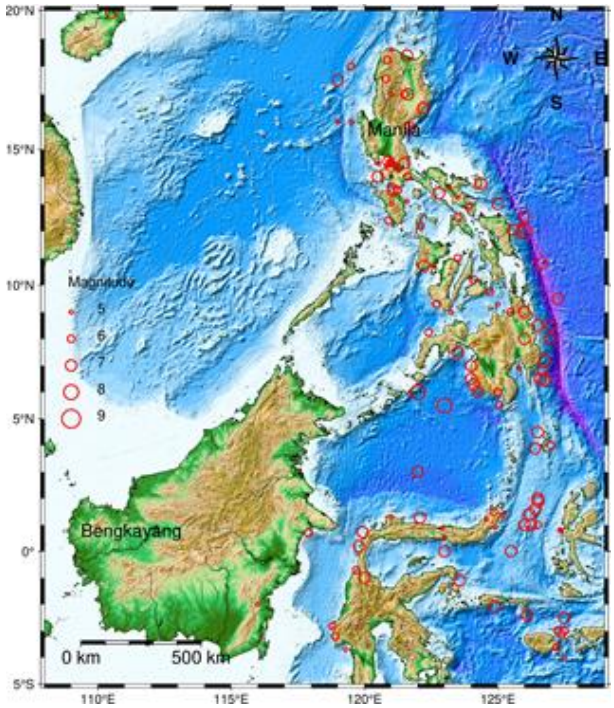

Fig. 4 Map of regional earthquake distribution for the period 1960-2022 (Sources: NOAA and IRIS).

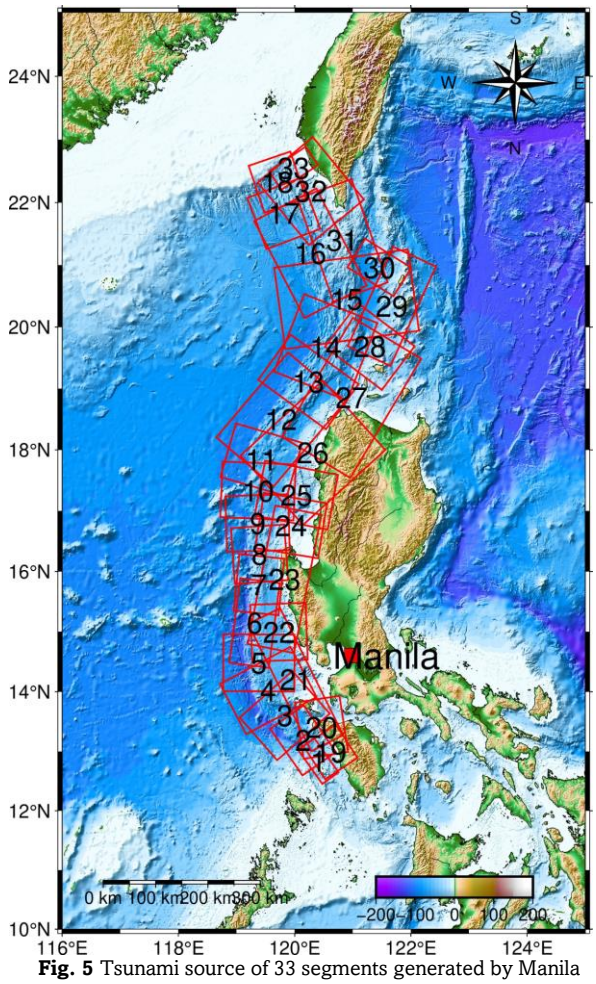

Fig. 5 Tsunami source of 33 segments generated by Manila trench.

PUSGEN revealed the presence of several faults on the island of Kalimantan. These include Meratus Fault in South Kalimantan, Mangkalihat Fault (East Kalimantan), Tarakan Fault (North Kalimantan), and Sampurna Fault, which passes near Sebatik Island. The Sampurna Fault is tertiary, runs from the Makassar Strait to the Paser area in East Kalimantan, trending southeast-northwest. Although an earthquake occurred in the Kendawangan area (West Kalimantan) on June 24, 2016, resulting in damage to several residential houses, the seismic activity in Kalimantan is generally not considered significant (Supartoyo, 2017).

Therefore, for the purpose of modeling, this study considers the earthquake potential for tsunamis using distant earthquake sources. We use a tsunami generator source with a purely tectonic scenario that is most likely to have an impact on the prospective nuclear reactor site at Gosong Beach, Kalimantan. We selected the most likely threat from the South China Sea (SCS) namely the Philippines tsunami source. We take reference from previous studies (Pribadi *et al,* 2021) by using a probabilistic approach from the occurrence of earthquakes around the Manila trench for a total of 33 segments which are then assumed to occur at the same time so that the accumulated results have a magnitude of M9.1 (Megawati *et al.,* 2009).

3. Result and Discussion

Tsunami modeling uses the Manila trench tectonic scenario, Philippines. Even though the generation using an earthquake is very large, the impact on the location of the nuclear power plant will not be too significant because the location is very far away, crossing the vast South China Sea, and being blocked by a series of small islands.

To consider and strengthen tsunami-resistant building construction, it is crucial to make a tsunami hazard forecast that closely aligns with potential future events. Previous modeling results indicate that West Kalimantan could experience a tsunami with a height of approximately 0.5 meters originating from the Philippine Trench fault source, similar to tsunamis reaching the Singapore Strait at 0.4-0.6 meters. Additionally, tsunami waves on the east coast of Malaysia can reach heights of 0.8 meters to 1 meter (Dao *et al.,* 2009; Megawati *et al.,* 2009). The latest modeling outcomes from Manila sources estimate a tsunami height of around 0.3-0.5 meters at the prospective Gosong beach site, with an estimated arrival time of approximately 550 minutes (9 hours 10 minutes) after the earthquake (Pribadi *et al.,* 2019). However, the previous modeling results did not use detailed topography and bathymetry because they only used free data, so the results were not optimal.

Tsunami modeling utilizing the Manila Trench source incorporates seven scenario domains, each producing distinct initial deformations that result in varying maximum tsunami heights as shown in Fig. 6(a) to Fig. 6(f). The maps used in domain 1 to domain 6 in Fig 6 use GEBCO, BATNAS, and DEMNAS data respectively. Tsunami generated by an earthquake with a Mw 9.1 in the Megathrust Subduction beneath the Manila Trench. The height of the tsunami is taken in the coastal area.

The first domain is in Fig. 6(a). The overall scope of this research location includes the Philippines and parts of Indonesia. The region is between 5° South and 20° North, and 108° East to 129° East. Tsunami height as high as 15 meters in the area of the earthquake source, the maximum simulated height value of the tsunami is in North Ilocos, Philippines around 24 meters.

The second domain is in Fig. 6(b) covers the South China Sea. Tsunami wave height is about 3 meters hitting the islands of Mindoro and Lubang in the Philippines (119.8° East, 13.5° North) and arriving at Northwest Sarawak, Malaysia with a wave height on the coast of about 2 m, while east of Phu Yen, Vietnam the wave height up to 5 meter. The results of the tsunami run up on the third domain of Fig. 6(c) show a tsunami wave height of 2 meters offshore around Mukah, Sarawak, Malaysia. The height of the tsunami waves shows a decreasing trend at the fourth domain of Fig. 6(d) is around height of covers the area around Kuching, Malaysia between 1.2 meters to 1.6 meters and the area around Sambas, Kalimantan, Indonesia between 0.8 meters to 1.5 meters.

The fifth domain of Fig. 6(e) covers the Singkawang area, West Kalimantan with a tsunami height of between 1 meter and 1.5 meters. The sixth domain of Fig. 6(f) is around the Bengkayang area with a tsunami height of between 0.6 meter and 1 meter. The outcomes are aggregated in a map displaying the maximum tsunami heights, enabling preliminary analysis of the significant tsunami propagation direction.

To understand the tsunami height at Gosong Beach and its vicinity comprehensively, can be seen in the seventh domain as the last domain with high resolution detailed topographic maps for each scenario. For the tsunami height in the Gosong Beach area as per the NPP site plan, which is the study location in Fig. 7, the highest tsunami wave height is between 0.3 meter to 1 meter.

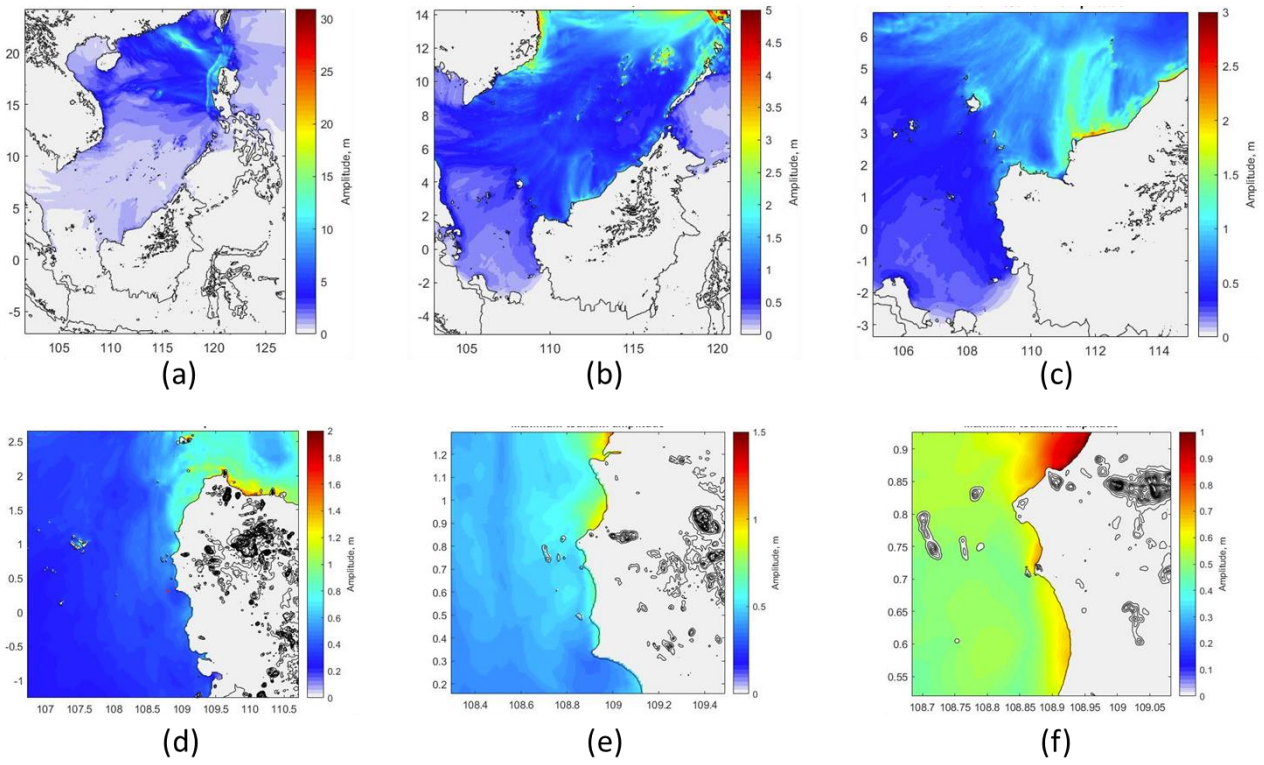

Fig.6 The tsunami modeling results at domain 1 (a), domain 2 (b), domain 3 (c), domain 4 (d), domain 5 (e), and domain 6 (f) utilizing the Manila Trench source.

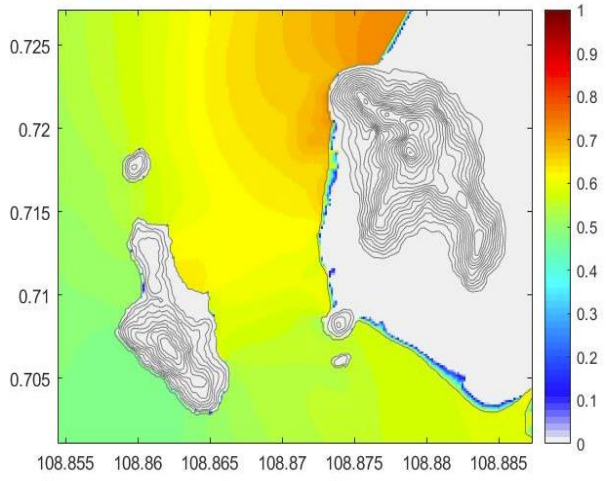

Fig. 7 The tsunami modeling results at domain 7 utilizing the Manila Trench source

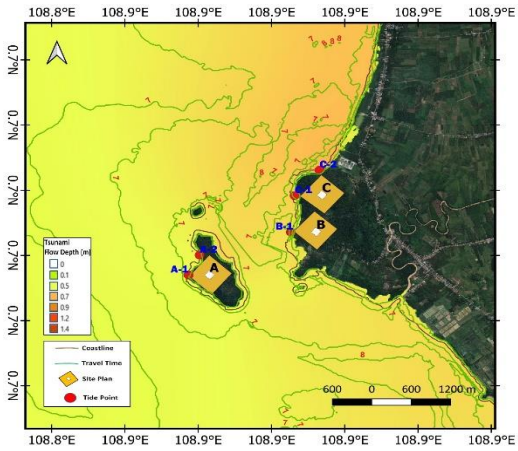

Fig. 8 The tsunami arrival time around Pantai Gosong.

Nuclear power plants in general have a generator system and cooling pipes. The nuclear system has at least a core thermal capacity of 4,451 MWt (Megawatt thermal). The Reactor Cooling System (RCS) functions to circulate hydrogen in a closed cycle, and removes heat from the core reactor (IAEA, 2020). The hydrogen in question is the volume of seawater on a large scale. The temperature of sea water coming out of the pipe is between 30 degrees to 40 degrees. Furthermore, it experiences cooling after circulating with wider sea water. The depth of sea water is 10 meters for the foundation of the water-cooling pipe. The path between the cooling pipes and the nuclear reactor must be small for safety reasons, and not affected by sea waves or turbidity currents. The design of the Pantai Gosong NPP for water cooling is paraded from the generator to a depth of 10 meters, which is between 1.5 kilometres and 2 kilometres following the design of the Bangka Strait opposite NPP to Southern Sumatra. The location has a depth of 10 meters for intake with the diameters of the pipe of 5 meters (1000 MWe) (Nugroho *et al,* 2021).

The site plan for nuclear power plant reactors in Bengkayang refers to a prior study (Mudjiono *et al.,* 2020). The initial placement of tide gauges, water cooling pipes, and other crucial bathymetric measurements was conducted at 12 points scattered across Gosong Beach in the north, center, and south. Additionally, several points were strategically positioned on

Table 2
The model results for time, height, and velocity in the x and y directions at the most potential site for NPP Bengkayang.

No	Lon, Lat (degree)	D (m)	Time (HH:MM)	h (m)	Vx (m/s)	Vy (m/s)
1	108.873, 0.712	0.6	9:23	0.58	0.34	0.46
2	108.871, 0.715	0.9	9:20	0.60	0.26	0.58
3	108.873, 0.720	0.7	9:24	0.62	0.15	0.48
4	108.867, 0.719	0.9	9:23	0.61	0.50	0.61
5	108.858, 0.706	1.6	9:10	0.48	0.31	0.48
6	108.859, 0.713	0.9	9:18	0.52	0.12	0.76
7	108.858, 0.708	0.7	9:17	0.49	0.12	0.36
8	108.860, 0.710	0.4	9:21	0.52	0.07	0.12
9	108.865, 0.707	0.2	9:24	0.56	0.02	0.42
10	108.863, 0.711	0.2	9:23	0.61	0.12	0.13
11	108.870, 0.703	1.5	9:24	0.55	0.32	0.49
12	108.874, 0.701	2.0	9:22	0.56	0.40	0.30

*) Annotation:
Lon : Longitude
Lat : Latitude
D : Depth
Time : Tsunami estimate arrival
h : Tsunami hight
Vx : Velocity axis X
Vy : Velocity axis Y

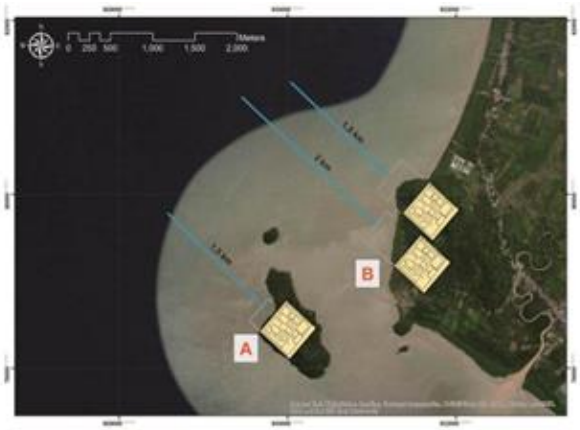

Fig. 9 The Bengkayang NPP site plan (Mujiono et al, 2020).

Semesak Island. The approximate location of the reactor placement plan is also illustrated in Figures 9 and 10 below.
Fig. 10 depicts the geomorphological conditions of both the land and sea at Gosong Beach. The initial tide gauge is represented by a transparent red triangle, while the location of the potential reactor is indicated by a yellow triangle. In Fig. 10(a), we illustrate the disparities between topographic and bathymetric maps in the final layer using only DEMNAS data with a resolution of 11 meters (Pribadi *et al.,* 2019), contrasting with the complete data presented in Fig. 10(b). In the Manila tsunami propagation area, other studies solely utilize GEBCO and ETOPO data, which have a coarse resolution and only cover the northern part of Borneo (Qiu *et al.,* 2019; Mardi *et al.,* 2015). This study provides assimilated maps incorporating DEMNAS, BATNAS, and field observation data, utilizing geodetic GNSS tools and UAV photography for local topography, as well as the Echosounder tool for measuring shallow sea depth.

The combined map reveals significant differences in detailed topographic heights. For lowland areas with elevations less than 10 meters, these results align with the actual ground conditions. The bathymetry demonstrates the depth of the shallow sea, ranging between 0 and 30 meters deep, visible along the coast and around the cluster of islands. A previous study presented model results at the outer tip of Semesak Island, indicating a tsunami height of 0.4 meters and an estimated time of arrival (ETA) of 9 hours and 36 minutes from the initial epicenter of the Manila Trench. The closest point to the prior location, number 5 to the west of Semesak Beach, exhibited a higher tsunami height of 0.48 meters with a faster arrival time of 9 hours and 10 minutes. Detailed results of the tsunami inundation model are presented in Table 2 and Fig. 8.

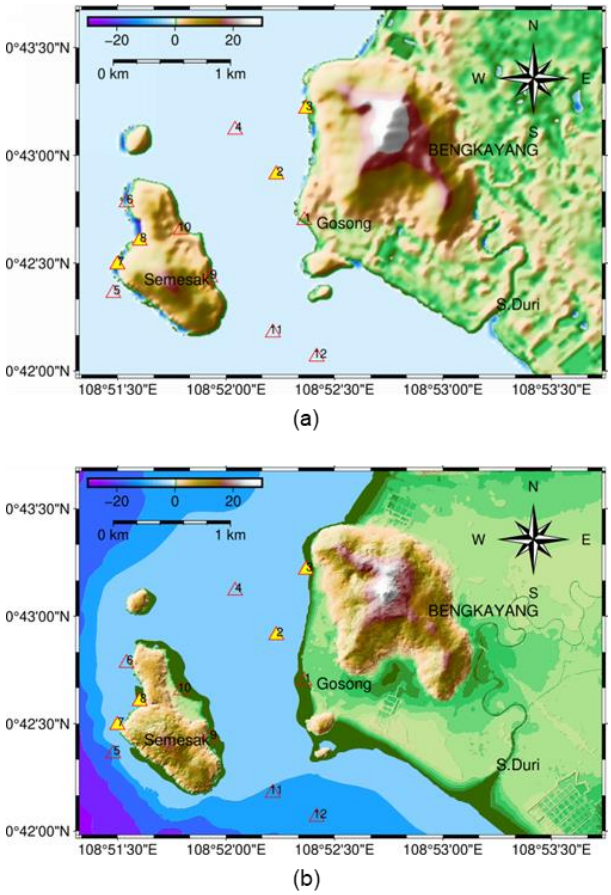

Fig. 10 Map of the initial tide gauge locations. (a) DEMNAS data, (b) a combination of BATNAS, DEMNAS, GNSS, UAV, and Bathymetry.

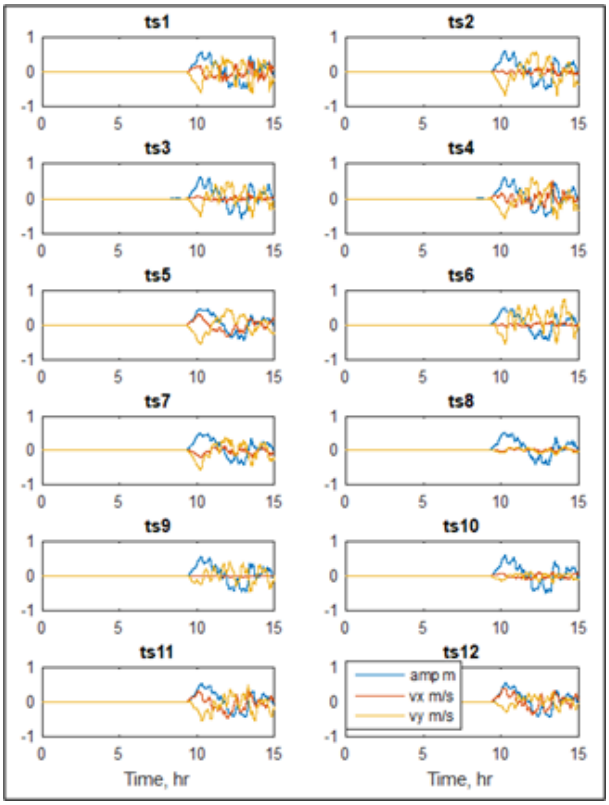

Fig 11. Initial waveform at water cooling location with detailed topography after tidal correction

Drawing on detailed topographic and bathymetric maps, inundation modeling yields optimal results following standard tsunami inundation map guidelines (Latief, 2013). This study addresses previous research with relatively coarse results due to the utilization of DEMNAS topography alone. Despite the homogeneity in bathymetric depth, the actual ground conditions are quite diverse. The altitude contours appear disorderly, portraying numerous high plains and cliffs along the coast. Subsequent field verification revealed extensive plains and vegetation. The combined observation map contradicts DEMNAS data that does not align with reality.

Synthetic waveforms were generated following preliminary testing and numerical modeling of tsunamis to depict the tsunami height and arrival time at virtual gauge locations. These synthetic waveforms provide a more detailed analysis of the tsunami's maximum height and arrival time at the designated virtual gauge points. Tsunami waveform as shown in Fig 11.

The analysis of results, employing detailed topographic maps, is anticipated to closely reflect actual conditions, given the incorporation of field data. Drawing on the insights of Griffin *et al.* (2015), the use of accurate data is crucial for achieving optimal and valid tsunami modeling results, especially concerning tsunami height and its arrival time at the shore. Validation of these results is feasible through field observations, as demonstrated by the 2006 Earthquake-Tsunami incident in Cilacap (Kongko, 2012), where the error or deviation was less than 20%. In this study, the analysis of tsunami results reveals that the highest tsunami was recorded on the west side of Semesak Island (number 3), reaching a height of 0.62 meters. Generally, within the last domain, tsunami heights range between 0.48 meters and 0.62 meters. Notably, these results surpass those of previous studies in the closest location, where heights ranged from 0.3 meters to 0.5 meters, a discrepancy

Table 3
Variation of tide in Bengkayang coastal area.

Variation of Tide	Value (m Above MSL)
Highest High-Water Level (HHWL)	0.944
Mean High Water Level (MHWL)	0.772
Mean Sea Level (MSL)	0.000
Mean Low Water Level (MLWL)	-0.772
Chart Datum Level (CD)	-0.843
Lowest Low Water Level (LLWL)	-0.944

attributed to the use of a coarse resolution (Pribadi *et al.,* 2021). Assuming the tsunami occurs under the HHWL condition as stated in Table 3, the tsunami height in the area will range from approximately 1.424 meters to 1.564 meters. This results in minimal damage to the coast and ship damage (Latief et al., 2003). In general, this location is quite adequate for the placement of water-cooling system instruments because it is under the foot of the hill at Gosong Beach. It is close to the location of the candidate reactor on the top of the hill and the cooling pipe with a bathymetry depth of 10 meters.

The arrival time for this study at a location west of Semesak Island (no. 5) was 9 hours 10 minutes. The time results are different from previous research values with an arrival time of 9,653 hours or 9 hours 39 minutes. This shows that the detailed topography affects the results of the estimated time of arrival (ETA). The previous observation point was outside Semesak Island, some distance from the current study. We estimate potential points for RCS placement north of Gosong Beach at no. 2 and no. 3, and west of Semesak Island at no. 7 and no. 8. Tsunami height in these points is around 0.49 meter to 0.62 meter. ETA is around 9 hours 17 minutes to 9 hours 24 minutes. Based on the tsunami classification from the Tsunami Hazard Map Technical Manual, this type of tsunami has the opportunity to experience an early warning (medium type) with a range of 0.5 meters to 3 meters (Latief, 2013).

For candidate water cooling sites, the resultant wave velocities for inundation range from 0.14 m/s to 0.79 m/s at depths between 0.2 and 2 meters, which is considered relatively safe to withstand the force of tsunami waves generated from the northern Philippines source. However, it is crucial for the cooling pipes to endure the compressive force exerted by the tsunami waves.

We recommend that the government, in planning the construction of the Bengkayang Nuclear Power Plant (NPP), incorporates a safety factor of 30% based on calculations from several worst-case tsunami scenarios, leading to an estimated tsunami inundation height at the potential location of the NPP reactor (FEMA, 2012).

4. Conclusion

To obtain a high-resolution map with detailed topography, the initial tide point displays the integration results between the BATNAS, DEMNAS, UAV maps, and field data of bathymetry and topography measurements. Besides that, the calculation domain is made up to the smallest scale grid up to the seventh domain. In general, the height of the tsunami from the source of the Manila trench is higher than the previous studies. The tsunami arrival time is faster than ETA of previous studies. This difference is due to better support for high-resolution data compared to previous studies with wide grids. The locations of Gosong Beach (no. 2 and no. 3) and Semesak Island (no. 7 and

no. 8) are considered the most potential for NPP placement because the locations are close to shallow seas making it relatively easy to install a water-cooling system.

Acknowledgments

The authors would like to thank for financial support being enabled by RISPRO LPDP and National Research and Innovation Agency (BRIN), Republic of Indonesia. Sponsorship Code: 2022 No. B-802/II.7.5/FR/6/2022 and B-9106/III.3/KS.0.0/9/2022. We would also like to thank COMCOT software developers and instructors, namely: Xiaoming Wang and Aditya Riadi Gusman. I would like to express my deepest appreciation to Heads of BMKG and BRIN and all related leaders so that this research can be completed on time.

Author Contributions: S.P., W.K., N.R.: Conceptualization, methodology, formal analysis, writing original draft, F., E.E.A., H.S., S.N., S.; supervision, resources, project administration, T.K., E.E.A.; writing—review and editing, project administration, validation. All authors have read and agreed to the published version of the manuscript.

Funding: This research was funded by RISPRO LPDP and National Research and Innovation Agency (BRIN). The author(s) received no financial support for the research, authorship, and/or publication of this article.

Conflicts of Interest: The authors declare no conflict of interest.

References

Alimah, S., Alhakim, E.E., Sunarko, Anzhar, K., Mudjiono (2021), Demographic Characteristics of Site Vicinity Area for Preparation in West Kalimantan NPP Site, *MIPI*, 15(2), 130-135, https://doi.org/10.29122/mipi.v15i2.4822.

BAPETEN (2018), Peraturan Badan Pengawas Tenaga Nuklir Nomor 4 Tahun 2018 tentang Ketentuan Keselamatan Evaluasi Tapak Instalasi Nuklir. Indonesia, https://jdih.bapeten.go.id/unggah/dokumen/peraturan/372-full.pdf

BAPETEN (2014), Peraturan Kepala Badan Pengawas Tenaga Nuklir Nomor 6 Tahun 2014 tentang Evaluasi Tapak Instalasi Nuklir Untuk Aspek Meteorologi dan Hidrologi, https://jdih.bapeten.go.id/unggah/dokumen/peraturan/279-1_(PERATURAN)-1597755443.pdf.

Blaser, L., Kruger, F., Ohrnberger, M., Scherbaum, F., 2010. Scaling relations of earthquake source parameters estimates with special focus on subduction environment, *Bulletin of the Seismological Society of America*, 100, 2914–2926, https://doi.org/10.1785/0120100111.

Bock, Y., Prawirodirdjo, L., Genrich, J. F., Stevens, C. W., McCaffrey, R., Subarya, C., Puntodewo, S. S. O., Calais, E, (2003), Crustal motion in Indonesia from Global Positioning System measurements, *J. Geophys. Res.*, 108, 2367. https://doi.org/10.1029/2001JB000324.

Costas, S., Utku, K. (2015), The fukushima accident was preventable, *Philosophical Transactions of the Royal Society*, A 373 (2053), 20140379, 1–23, https://doi.org/10.1098/rsta.2014.0379.

Dao, M.H., Tkalich, P. (2007) Tsunami propagation modeling - a sensitivity study. *Natural Hazards and Earth System Science,* 7(6), 741–754, https://doi.org/10.5194/nhess-7-741-2007.

Diposantono, S., and Budiman. (2006), Tsunami, *Buku Ilmiah Populer*, Bogor.

Federal Emergency Management Agency (FEMA) (2012), Guidelines for Design of Structures for Vertical Evacuation from Tsunamis, FEMA P-646/April 2012.

Global Historical Tsunami Database, National Oceanic and Atmospheric Administration (NOAA) (http://ngdc.noaa.gov), https://doi:10.7289/V5PN93H7.

Griffin, J., Latief, H., Kongko, W., Harig, S., Horspool, N., Hanung, R., Rojali, A., Maher, N., Fuchs, A., Hossen, J., Upi, S., Dewanto, S.E., Rakowsky, N. and Cummins, P. (2015), An evaluation of onshore digital elevation models for modeling tsunami inundation zones. *Front. Earth Sci.* 3, 32, https://doi.org/10.3389/feart.2015.00032.

Hakim, F.S.N., and Setijadi, R. (2021), Karakteristik Batuan Mesozoikum di Daerah Bengkayang: Berdasarkan Kandungan Unsur Anorganik, *Jurnal Geologi dan Sumberdaya Mineral*, 22(1). https://doi.org/10.33332/jgsm.geologi.v22i1.

IAEA (2020), Advanced Large Water Cooled Reactors, A Supplement to: IAEA Advanced Reactors Information System (ARIS), *International Atomic Energy Agency (IAEA)*, https://www.iaea.org/topics/water-cooled-reactors.

Kajiura, K., & Shuto, N. (1990). Tsunami in the sea, Edited by B. Le Mehaute and D.M. Hanes number 9 part B. 395-420. *John Wiley and Sons, Inc.*

Kongko, W. (2012), South Java tsunami model using highly resolved data and probable tsunamigenic sources. Hannover : Gottfried Wilhelm Leibniz Universität, *Dissertation,* 347 S, https://doi.org/10.15488/7888.

Latief, H., Hadi, S., Sunendar, H., Gusman, A.R., (2003), Tsunamis Assement Around The Sunda Strait, International Seminar/Workshop on Tsunami "In Memoriam 120 years of Krakatau Eruption –Tsunami and Lesson Learned from Large Tsunami", Jakarta.

Latief, H. (2013), Pedoman Teknik Peta Rawan Bahaya Tsunami, Badan Nasional Penanggulangan Bencana, https://perpustakaan.bnpb.go.id/bulian/index.php?p=fstream&fid=253&bid=1901.

Lipscy, P.Y., Kushida, K.E., Incerti, T. (2013), The Fukushima disaster and Japan's nuclear plant vulnerability in comparative perspective, *Environ Sci Technol,* 47(12), 6082-8. https://pubs.acs.org/doi/10.1021/es4004813.

Liu, Y. G, Steg, A, Smits, B, Tamminga, S, (1994), Crambe meal: removal of glucosinolates by heating with additives and water extraction. *Anim. Feed Sci. Technol.*, 48 (3-4), 273-287, https://doi.org/10.1016/0377-8401(94)90178-3.

Mansinha, L. & Smiley, D.E., 1971. The displacement field of inclined faults, B. seism. Soc. Am., 61, 1433–1440, https://engineering.purdue.edu/~ce597m/Handouts/The%20displacement%20fields%20of%20inclined%20faults.pdf

Matsutomi, H., Okamoto, K., Harada, K. (2010), Inundation flow velocity of tsunami on land and its practical use, *Coastal Engineering Proceedings*, https://doi.org/10.9753/icce.v32.currents.5.

Megawati, K., Shaw, F., Sieh, K., Huang, Z., Wu, T., Lin, Y., Tan, S. K., and Pan, T. (2009), Tsunami hazard from the subduction megathrust of the South China Sea: Part I. Source characterization and the resulting tsunami, *Journal of Asian Earth Sciences*, 36, 13-20, https://doi.org/10.1016/j.jseaes.2008.11.012.

Mudjiono, Alimah, S., Susiati, H., (2020), Identifikasi Perubahan Tataguna Lahan di Sekitar Calon Tapak PLTN Kabupaten Bengkayang, Kalimantan Barat, *Jurnal Pengembangan Energi Nuklir* 22(2), http://dx.doi.org/10.17146/jpen.2020.22.2.6120.

Nugroho, A., Kusratmoko, E., and Indra, T.L. (2021), Preferred Site Selection Using GIS and AHP: Case Study in Bangka Island NPP Site, *Jurnal Pengembangan Energi Nuklir,* 23(1), 51-60, http://dx.doi.org/10.17146/jpen.2021.23.1.6404.

Omoto, A. (2015), Where was the weakness in application of defense-in-depth concept and why? Reflections on the Fukushima Daiichi Nuclear Accident, towards Social-Scientific Literacy and Engineering Resilience, Springer Open, Springer Cham Heidelberg, Germany, Ch. P131-164, https://doi.org/10.1007/978-3-319-12090-4_8.

PP (2014), Peraturan Pemerintah Nomor 79 Tahun 2014 tentang Kebijakan Energi Nasional, https://jdih.esdm.go.id/peraturan/PP%20No.%2079%20Thn%202014.pdf.

Pribadi, S. Afnimar, Puspito, N.T., Ibrahim, G. (2013), Characteristics of Earthquake-Generated Tsunamis in Indonesia Based on Source

Parameters Analysis, *Journal of Mathematical and Fundamental Sciences*, https://doi.org/10.5614/j.math.fund.sci.2013.45.2.8.

Pribadi, S., Fauzi, Kurniawan, T., Sunarko, Suntoko, H., Sudrajat, A., Prayitno, B.S., Riama, N.F. (2021), Manila Trench Tsunami Source Modeling for West Kalimantan Nuclear Facility Mitigation, *Journal of Physics: Conference Series*, https://doi.org/10.1088/1742-6596/2019/1/012082.

PUSGEN (2018), Pusat Studi Gempa Nasional, Peta Sumber dan Bahaya Gempa Indonesia Tahun 2017, *Pusat Penelitian dan Pengembangan Kementerian Pekerjaan Umum dan Perumahan Rakyat*, ISBN 978-602-5489-01-3.

Schloderer, G., Bingham M., Awange, J.L., Fleming, K.M, (2010), Application of GNSS-RTK derived topographical maps for rapid environmental monitoring: A case study of Jack Finnery Lake (Perth, Australia), *Environ Monit Assess 180,* 147–161. https://doi.org/10.1007/s10661-010-1778-8.

Schlurmann, T., Kongko, W., Goseberg, N., Natawidjaja, D.H., Sieh, K (2011), Near-field tsunami hazard map Padang, West Sumatra: Utilizing high resolution geospatial data and reasonable source scenarios, *Coastal Engineering Proceedings*, https://doi.org/10.9753/icce.v32.management.26.

Suntoko, H., Sunarko, Susiati, H., Suryanto, S., Rudi, E., Raharjo, P., Karakteristik Pantai Dan Proses Geologi di Pantai Gosong, Kab. Bengkayang, Kalimantan Barat, *JPEN*, 23(2), 119-127, http://dx.doi.org/10.17146/jpen.2021.23.2.6553.

Supartoyo. (2017), Ancaman dan Potensi Gempabumi di Kalimantan, Prosiding Pertemuan Ilmiah Tahunan Riset Kebencanaan Ke 4,1-13, Depok: Universitas Indonesia.

UU (2007), Undang-Undang Negara Republik Indonesia No. 24 Tahun 2007 tentang Penanggulangan Bencana.

Wang, X. and Power, W. (2011). COMCOT: a Tsunami Generation Propagation and Run-up Model, *GNS Science Report*, 2011/43,129 pp., 2011.

Webb, P. (2017), Introduction to Oceanography. Online OER textbook. https://webboceanography.pressbooks.com